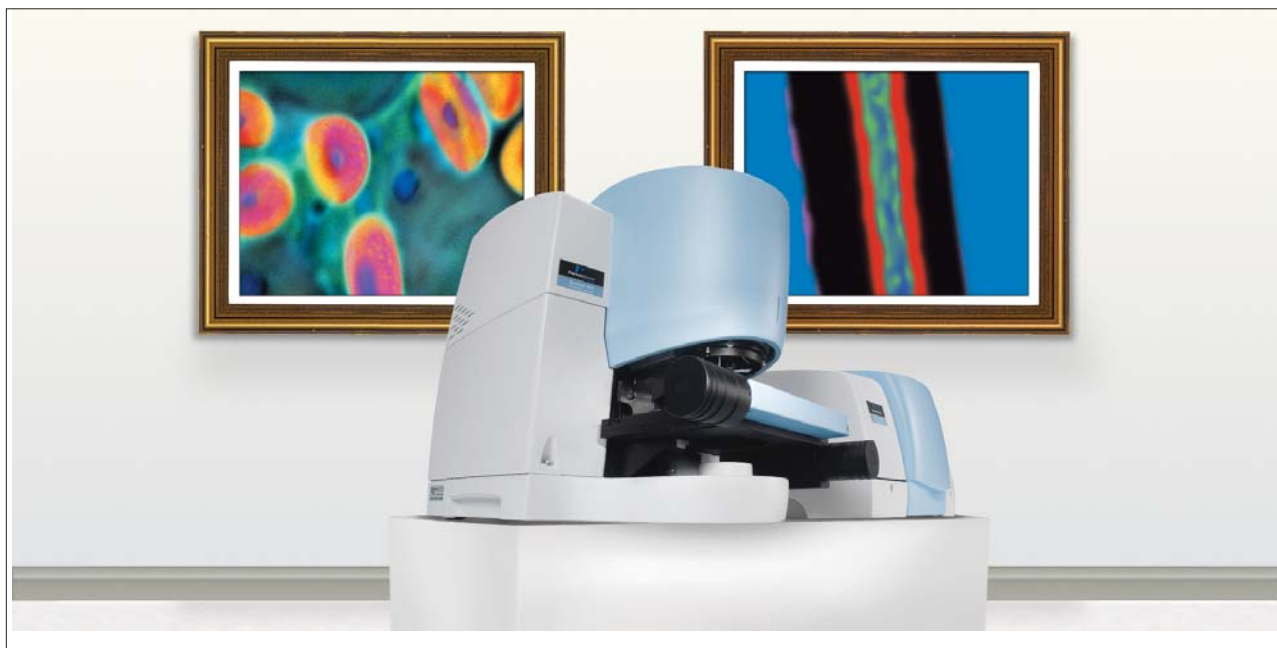


ATR Imaging of Pharmaceutical Tablets



Introduction

There has been a significant and growing interest in chemical imaging of pharmaceutical tablets in recent years. Technology improvements and increased use has established chemical imaging as a means of providing information on certain critical quality parameters that is not readily addressable using other techniques. In addition to major pharmaceutical manufacturers, generic manufacturers and even regulatory authorities¹ now recognize the value of chemical imaging both in troubleshooting in manufacturing and scale-up and in root cause analysis². Of the various imaging techniques, NIR

imaging has probably (and justifiably) received most attention, and is poised to grow further as a PAT-enabling technique³. Other chemical imaging techniques such as Raman and mid-IR diffuse reflectance each have their own merits and disadvantages, but NIR is attractive from the technology, implementation and sampling perspectives. Data generated by this method is also more familiar to many users in this area who might have experience in macro-NIR spectroscopy of tablet ingredients. That said, NIR imaging using current technology (be it FT, tunable or fixed filter) suffers some intrinsic

limitations due to the nature of the measurement itself, not the technology *per se*. First, the sample penetration by the incident light is relatively deep (many tens of microns) and the resulting image is effectively smeared out by the nature of diffuse reflectance. We estimate that the sample penetration is at least this order (dependent on particle size, packing and other parameters), yet we also know that many tablet ingredients are introduced into the blender with a particle size of less than 10 microns. So the technique must be sub-optimal for the purpose of generating sharp, distinct, pure,

ingredient images which show the ingredient's spatial distribution unless these ingredients form aggregates. Of the publications on NIR imaging, to the author's knowledge, no publication has shown particle size distributions for single particles of less than 10 microns in size. The examples tend to focus on showing aggregates of small particles or larger particles of many tens or hundreds of microns in size, yet particles of less than 10 microns must exist in the distribution. It is also known that for certain ingredients, such as magnesium stearate, the component is sometimes difficult to detect with NIR imaging even at relatively high concentrations unless it forms aggregates of ca 30-40 microns or larger, due to the distribution of the material throughout the matrix as relatively fine particles. Indeed, some actives at the sub-percent level are not seen at all unless they are present as aggregates. Second, the measured NIR spectra in images tend to be highly overlapped. In macro-NIR spectroscopy, NIR spectra are generally less discriminating than their corresponding Raman or mid-IR counterparts and this disadvantage is compounded in NIR imaging, where signal to noise ratios tend to be lower than on the macro-scale. The result of these two factors is increased reliance on chemometric analysis of the spectral data in the image. Moreover, subsequent image analysis also uses pixel counting statistics, which often depend on the requirement to classify individual image pixels as belonging to one chemical class or other. In practice, this represents a difficult step in the analysis when it is known that one rarely observes pure component spectra at single pixels in NIR images. This renders the overall image analysis more difficult in the NIR as the decision in

assigning a '1' or '0' to a gray-scale pixel is often somewhat subjective.

ATR imaging in the mid-IR offers the opportunity to provide some major advantages in this application relative to other techniques.

Compared with NIR imaging, it offers a large improvement (ca an order of magnitude) in spatial resolution – now of the order of the individual particle sizes of many ingredients (less than 10 microns) when they are introduced into the process. Better than 5 microns spatial resolution⁴ has been demonstrated with ATR imaging. Second, the spectra in the images tend to be of very high contrast, and more easily discriminated than in NIR. Third, the technique is effectively a surface technique, with a sample penetration depth of ca 1-2 microns, using the optical arrangement described below. The result is that individual pixel spectra are relatively more pure and the burden on the subsequent image analysis is lower than in NIR. There is no reason why some of the techniques used in hyperspectral NIR image analysis cannot be used for ATR images. Other advantages of ATR include the fact that large commercial libraries are available and may be used for qualitative identification, and some materials that are difficult to identify with NIR, such as some anhydrous inorganic salts, give high contrast ATR spectra.

We have developed an ATR accessory for the PerkinElmer® Spotlight™ 300 and 400 imaging systems and measured a number of pharmaceutical tablets. This note describes ATR imaging measurements of commercial pharmaceutical tablets and demonstrates a number of the advantages described above. As such, this technique shows a major

advance in state of the art pharmaceutical tablet imaging. Although, still at the 'infancy' stage, it is expected to grow and to play a very significant role in future pharmaceutical tablet and blend analysis.

Experimental

Sample Preparation and Presentation

For this study, whole uncoated pharmaceutical tablets (both prescription drugs and over-the-counter - OTC) were obtained along with samples of the raw ingredients known to be present in the tablets. For the prescription product, the ingredients were active, microcrystalline cellulose, calcium phosphate dibasic, starch and magnesium stearate. For the OTC product, the raw ingredients were aspirin, paracetamol, caffeine and a number of organic and inorganic minor ingredients. In this instance, the tablets were 2-3 mm thick, with vertical sides and flat surfaces. It was not necessary to perform any special milling/cutting on the surfaces, although this would be required for curved surfaces (this is one limitation of the ATR technique).

The ATR accessory comprises a germanium crystal with a conical cross section, Figure 1. The tip of the crystal is pressed into the tablet surface. The accessory is designed such that the sample region of interest (ROI) can be located using the visible microscope camera and the ATR sampling surface brought down onto the ROI without moving the sample. The crystal tip allows a circular sampling area of diameter ca 0.5 mm in which various sizes of square or rectangular image can be defined. Given an image pixel size of 1.56 microns, an area of 500 x 500

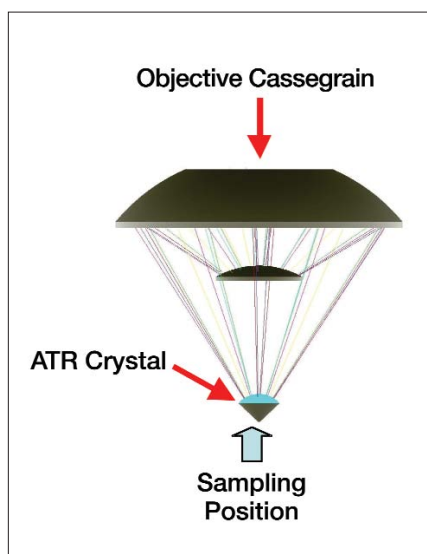


Figure 1. ATR sampling configuration.

microns would contain more than 102000 individual spectra.

In order to perform the most thorough image analysis, it may be necessary to obtain reference ATR spectra from the raw ingredients of the tablet. For best results, the spectra should be measured using the ATR imaging system, as opposed to extraction from standard reference libraries, although the latter may be used with some degradation in the image analysis. In this study, simple micro-disks were prepared for each of the raw ingredients of the

tablets using a standard KBr micro-pellet accessory commonly used in IR spectroscopy. Using a standard micro-pellet (2 mm die) accessory, hand-pressure is sufficient to generate a disk for ATR data collection. Once pressed, the disks are transferred to the ATR accessory and small images (50 x 50 microns) of the pure components are measured. From these images, single reference spectra are computed using the Spotlight software. Collection of reference images takes a few minutes per ingredient. This operation is generally performed only once.

Imaging

Images were collected using a standard PerkinElmer Spotlight mid-IR imaging system equipped with an ATR imaging accessory. The system uses a small MCT detector array combined with a moving sample stage/ATR accessory to generate images. The ATR crystal is clamped to the sample and does not move relative to the sample – the entire assembly of sample and ATR crystal are moved relative to the IR detectors. Image pixel size is 1.56 x 1.56 microns (6.25 x 6.25 microns pixel size is also available) and a spectral resolution of 16 cm⁻¹ was

used for the images. For this study, actual image sizes varied from 100 x 100 microns to 400 x 400 microns with total image collection times varying from 1 minute to ca 40 minutes.

Image data processing included spectral derivatisation, normalization and principal components analysis, and least squares full spectrum curve fitting performed using the PerkinElmer Hypersoft 3.0 software. Some further graphical image enhancement and statistical analysis was performed using ImageJ Version 1.36b public domain image processing and analysis software⁵.

Results and Discussion

A visible image from a tablet surface is shown in Figure 2a. Although it is possible to discern some granules in the visible image, there is no effective way of assigning the particles to individual ingredients from the visible image alone. Figure 2b on the other hand shows how the starch component is distributed. This was derived from the ATR image following a number of data processing steps which will be outlined in this section. Individual ingredient distribution patterns may be derived in a similar manner, allowing a

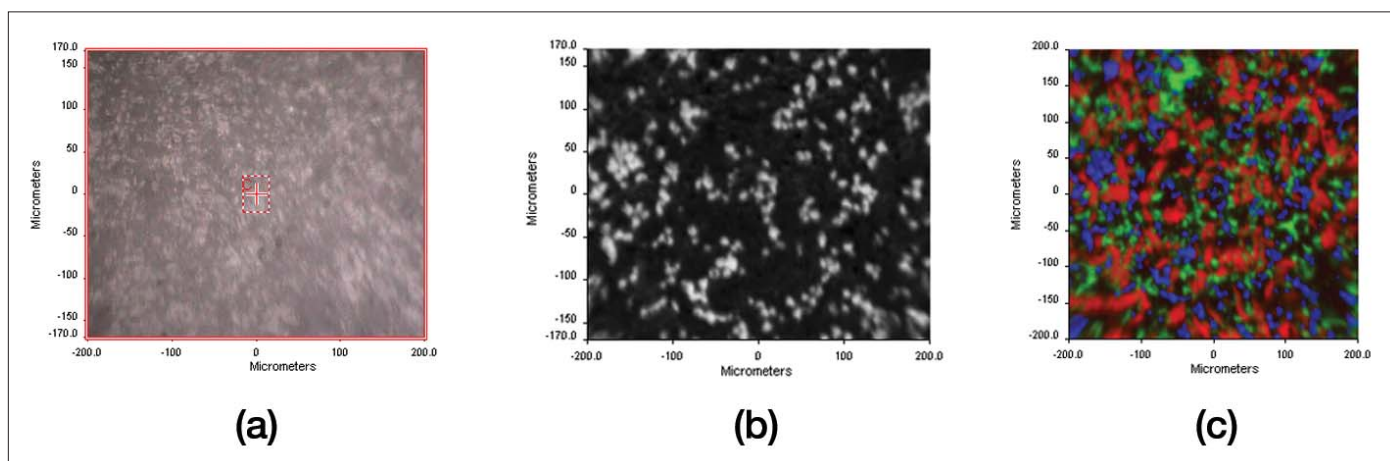


Figure 2. Visible (a), derived single component IR image (b) from tablet surface and (c) composite image from 3 major components.

composite image to be constructed. In this case, the three major components were merged to a single RGB (red/green/blue) composite image (Figure 2c). This kind of representation is common in NIR imaging of these products. What is different in this measurement is the much improved spatial resolution compared with NIR imaging and the higher degree of spatial contrast between image pixels to yield sharper, more detailed images from the tablet surface—in relatively short measurement times, and the ability to locate domains which are currently not detectable using NIR imaging.

Raw Ingredients Spectra

Figure 3 shows the ATR spectra of the raw ingredients for a tablet, alongside their corresponding first derivative spectra. With ATR imaging, it is observed that the field of illumination is not entirely flat across the entire face of the crystal element, and this manifests itself primarily as a smooth baseline offset variation in spectra measured across the crystal area. To a first order, this is easily handled by working with first or second derivative spectra. One point to note is in comparison with NIR imaging, the spectra of the ingredients are very distinctive, offering a greater possibility for more simple univariate approaches to the image analysis. For testing purposes, a common raw ingredient, povidone, known *not* to exist in the tablet, was added as a test raw ingredient to illustrate the effectiveness of the subsequent data processing.

Testing for the Presence of Tablet Ingredients

The first step is to confirm the presence of spectral contributions from the raw ingredients in the

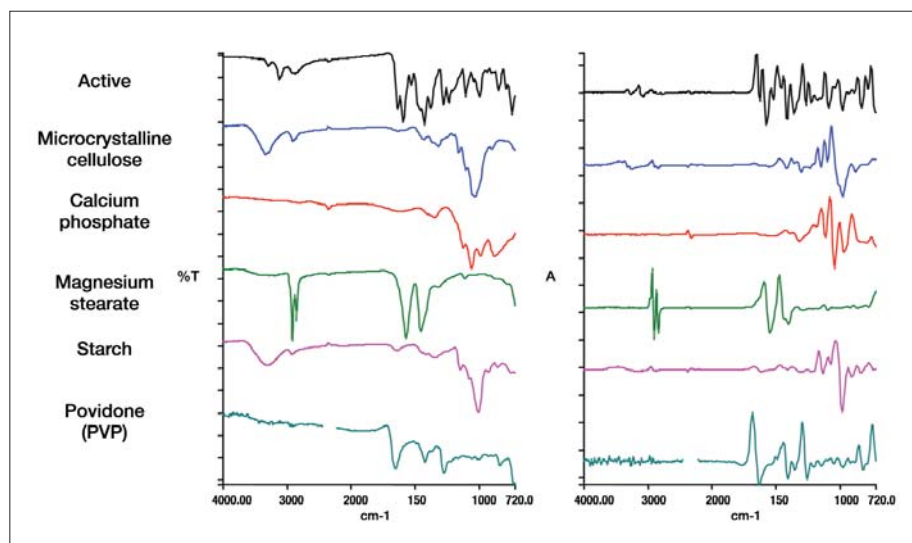


Figure 3. Suspected raw ingredients.

image spectra. This was performed using the 'Target' function in the Hypersoft software. The spectra in the image are pre-processed (first derivative, and blanked in the regions of CO₂ absorption) and a principal components analysis (PCA) of the spectra performed to extract the major independent spectra contributions. The raw ingredient or 'target' spectra are then fitted to linear combinations of the principal components from the PCA. The closeness of fit gives an indication of whether the target spectra are present in the image spectra. The results for the five components of the tablet are shown in Figure 4. The quality of fit for all five of the ingredients was excellent whereas the quality of fit for the povidone was poor, reinforcing the validity of this method.

Estimating Individual Ingredient Distributions in the Tablet

Having confirmed that the target spectra are present in the image spectra, the next step is to estimate the relative abundance of the ingredients at each pixel in the image to generate the individual

component distribution maps. There are a number of approaches to this, but for a five component mixture with the assumption of no chemical interaction between the components and the pure raw ingredient spectra available, a simple full spectrum curve fitting is found to work well. Having examined the residual image after the principal components analysis above to check for any additional chemical components present, each pixel spectra is simply modeled as a linear combination of the raw ingredient spectra. This technique can be less reliable if strong cross correlations exist between the target spectra; that is if some of the target spectra have many peaks in common. In this example, there is clearly some correlation between the spectra of microcrystalline cellulose and starch – but they are still sufficiently different to enable a well-conditioned least-squares curve fitting. Figure 5 shows the results for the spectrum curve fitting for the five ingredients. In each image, the pixel intensity shows the relative abundance of the target spectra in the image spectra.

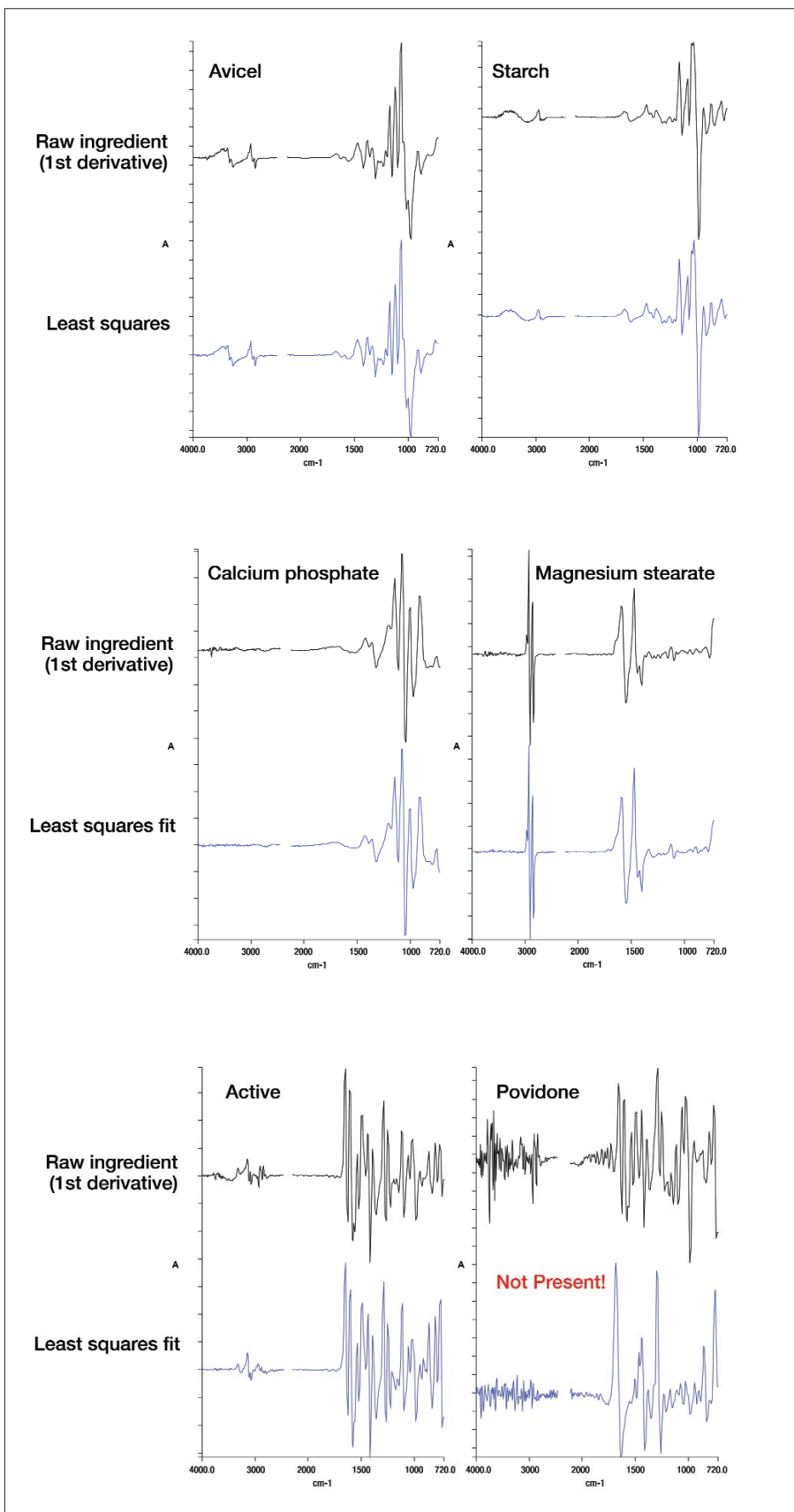


Figure 4. Testing for presence of raw ingredients.

In most cases, the ‘hot’ spots in the derived images contain spectra like those of the pure components spectra, with ‘mixture’ pixels around the edges of the particles, as expected. Typical spectra from the hot spots are illustrated in the figure, along with the corresponding raw ingredient spectra. There are three interesting points to note in these images.

- The spectral contrast and hence sharpness is remarkable – far sharper than most NIR counterparts. This is easily seen by plotting the histogram distributions in the images.
- The shapes of the hot spots (particles) are not only different for the different ingredients, but are actually starting to appear similar to those of the raw ingredients. For example, scanning electron microscope (SEM) images for starch particles are shown in Figure 6a, where the starch particles are seen to be highly spherical, unlike many other ingredients. The corresponding derived ATR image, Figure 6b, shows particles with similar shape. Similarly, the magnesium stearate and microcrystalline cellulose domains tend to have highly irregular shapes not unlike the SEM images for the raw ingredient. This observation, arising from the improved fidelity of the image compared with NIR, could provide very important additional information in assisting understanding the spatial distributions and correlating with product quality attributes.
- Individual particles smaller than 10 microns can be discerned. Figure 7 shows an expanded area from the calculated distribution for the active ingredient, known

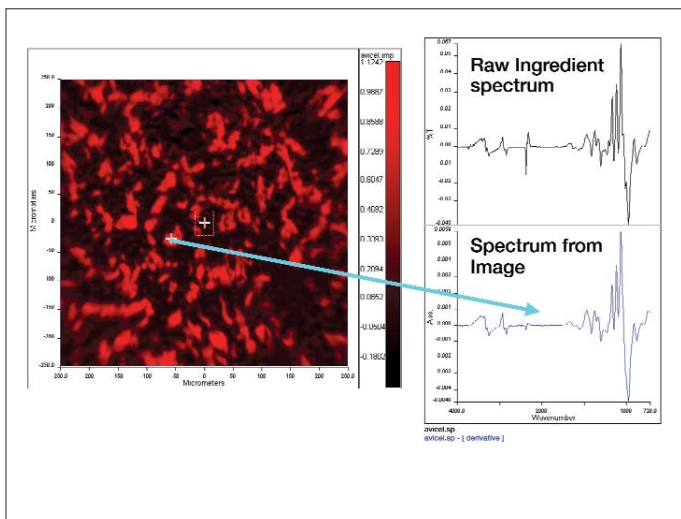


Figure 5a. Least squares fitted image for microcrystalline cellulose.

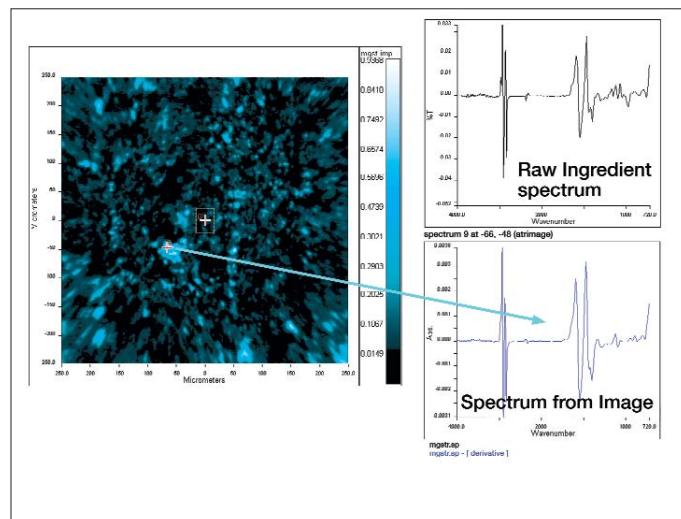


Figure 5d. Distribution for magnesium stearate.

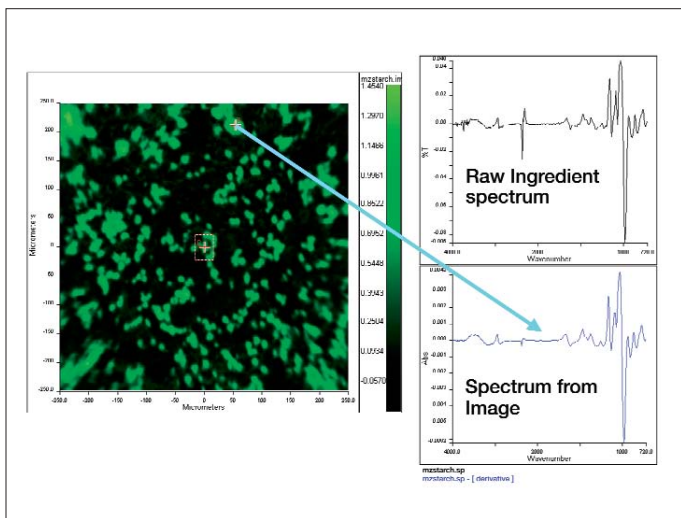


Figure 5b. Distribution for starch.

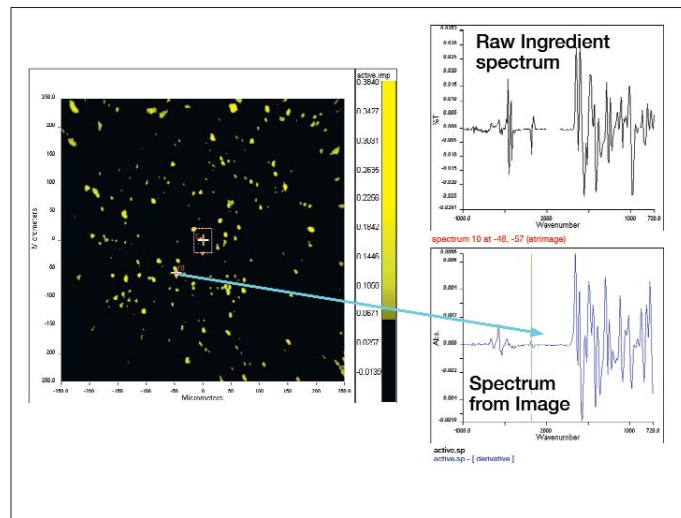


Figure 5e. Distribution for active (< 1%).

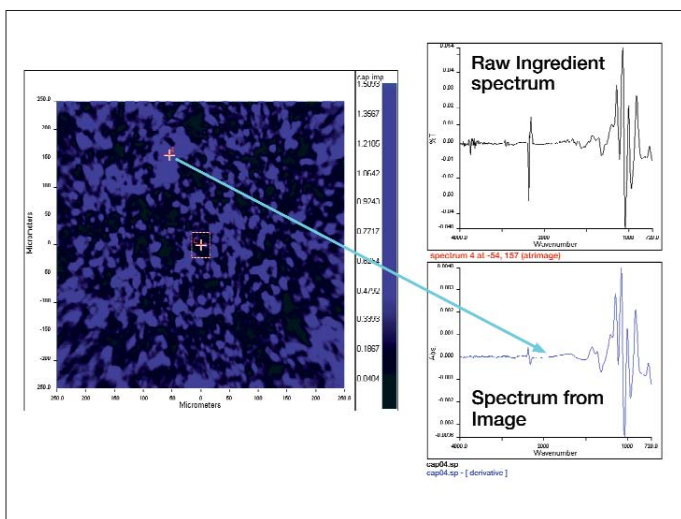


Figure 5c. Distribution for calcium phosphate.

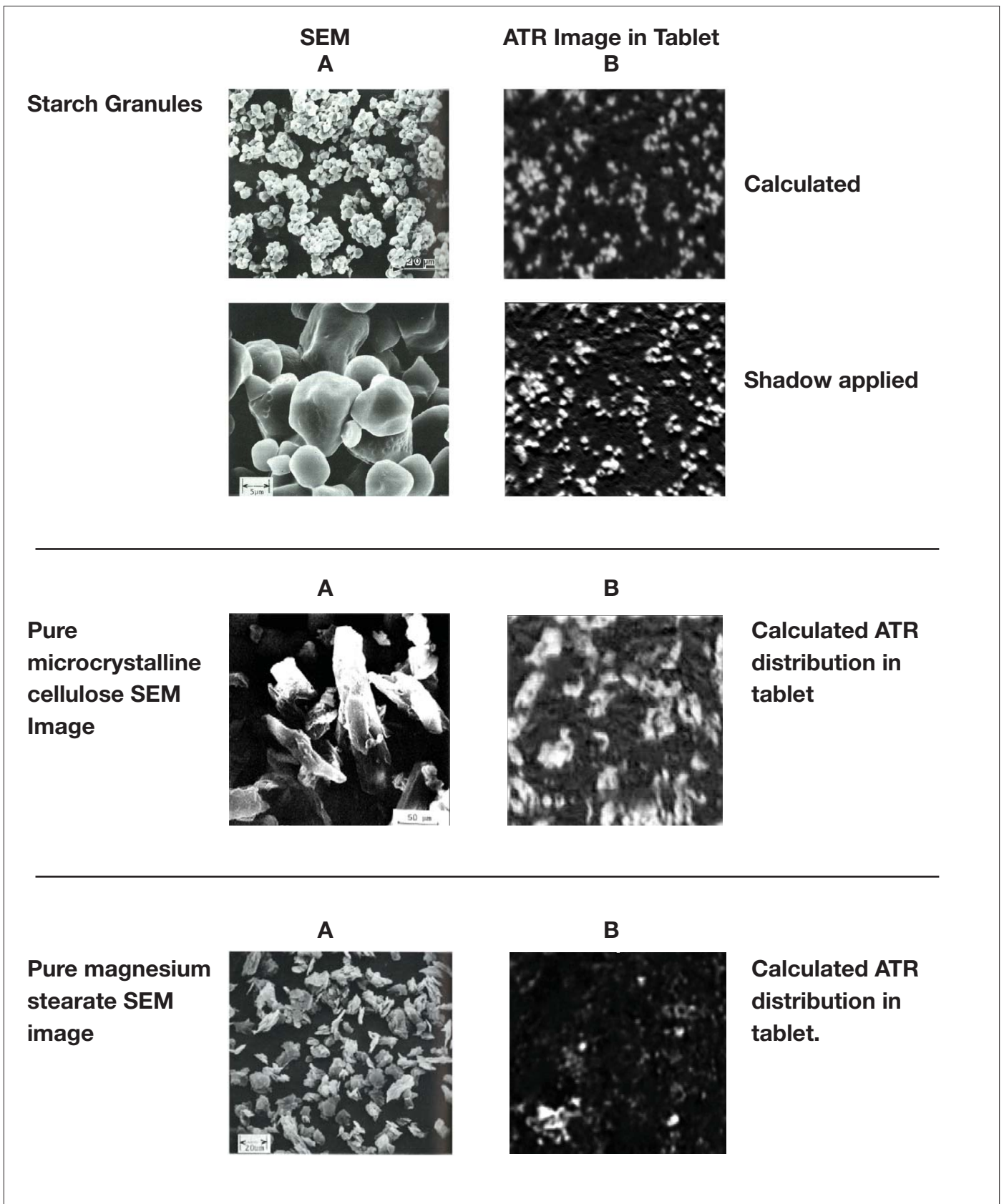


Figure 6. ATR particle image shapes-comparison with SEM.

to be present at less than 1% concentration by weight. The area shows hot spots around 6-7 microns in diameter. From the spectra measured at the hot spots, it is apparent that many pixels contain almost pure active spectra. It is worth noting that separate resolution studies⁶ estimate the spatial resolution of the technique to be of the order of 3-4 microns at ca. 1700 cm⁻¹. Again, the

spectral clarity from single particles is striking.

A second example showing resolution of small particle sizes is shown in Figure 8. Here, an OTC soluble analgesic tablet was imaged. A number of NIR imaging examples use this kind of product to demonstrate the capabilities of NIR imaging. The major ingredients, aspirin, paracetamol and caffeine are located

as large domains many tens or even hundreds of microns in diameter. However, the example here images not only the major components above, but a number of minor ingredients present (a) at low levels and (b) more importantly with domain sizes of less than 10 microns. Many excipients and APIs are introduced with particle sizes of less than 10 microns. NIR imaging does not easily detect individual particles of this size but rather, domains where these particles have formed aggregate of much larger size. Here, the figure shows not only the major ingredients, but in addition, individual calcium phosphate particles contained within the aspirin/caffeine/paracetamol distribution where the individual particles are not seen by NIR.

Characterizing Tablet Ingredient Distributions

With high quality individual ingredient distributions like those displayed in Figure 5, the eye can see obvious differences between different ingredients in a tablet. However, if a more rapid, less subjective characterization is required, it is necessary to express the images in different manner. One way is to express the images as histograms of intensities of the image. Usually, for a given image, the pixel brightness is plotted against the number of pixels and the resulting histogram can be analyzed to provide useful information which has been related to key tablet process parameters. With sharp ATR images, when an ingredient distribution is plotted as such, the resulting histogram usually has two distinct modes corresponding to the particles of interest and the remainder Figure 9a. However, the borderline between the two zones of the

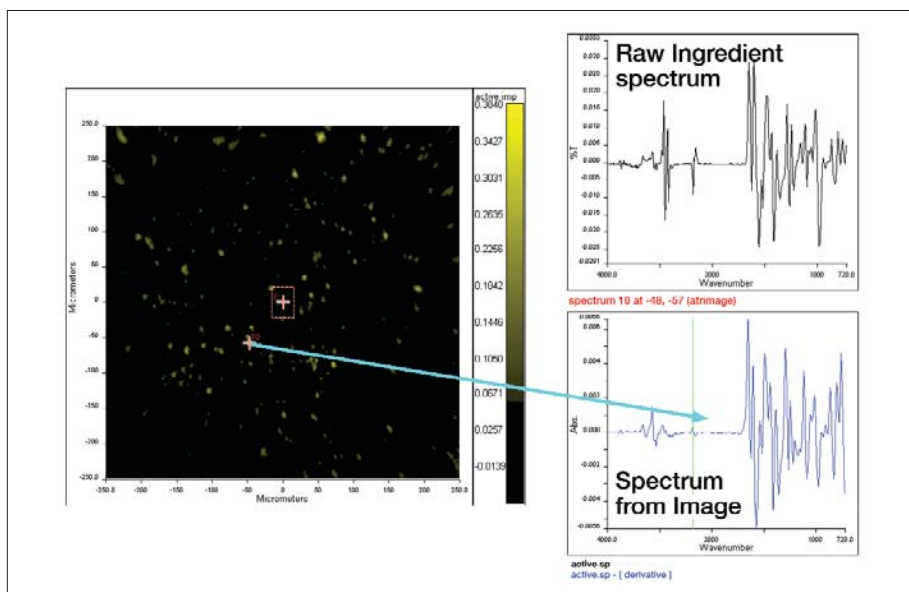


Figure 7a. Distribution for active (< 1%).

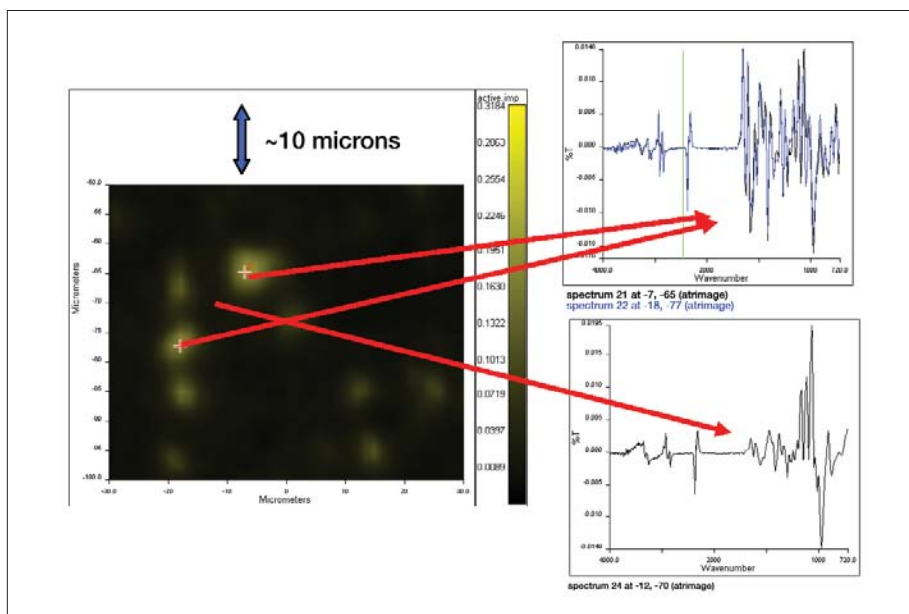


Figure 7b. Active ingredient particles < 10 microns.

histogram is not always distinct. Since the image is a grayscale image, there will be a number of pixels which fall between 'pure' particle pixels and 'pure' background pixels. For pixel counting,

these pixels need to be assigned as foreground or background pixels, i.e. an intensity threshold must be set above which pixels are assigned to the particles of interest, and below which particles are assigned

to the remainder or background. There are some mathematical recipes for estimating this threshold, e.g. 'maximum entropy method'⁵, or it may be estimated subjectively. For ATR images, it has

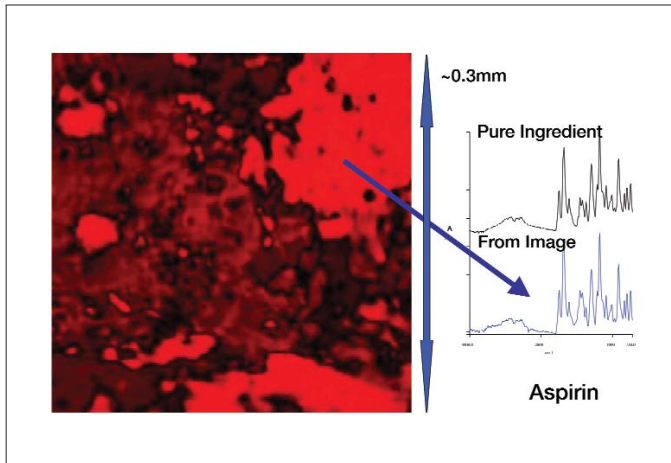


Figure 8a. Analgesic tablet – coarse structure - aspirin.

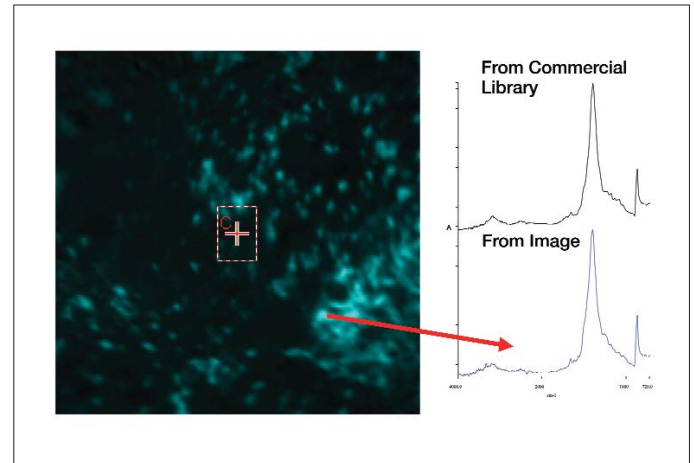


Figure 8d. Revealing minor constituents – calcium carbonate.

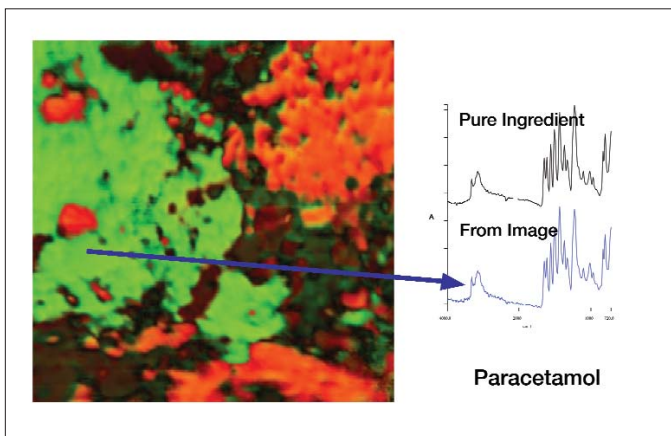


Figure 8b. Overlaying paracetamol distribution.

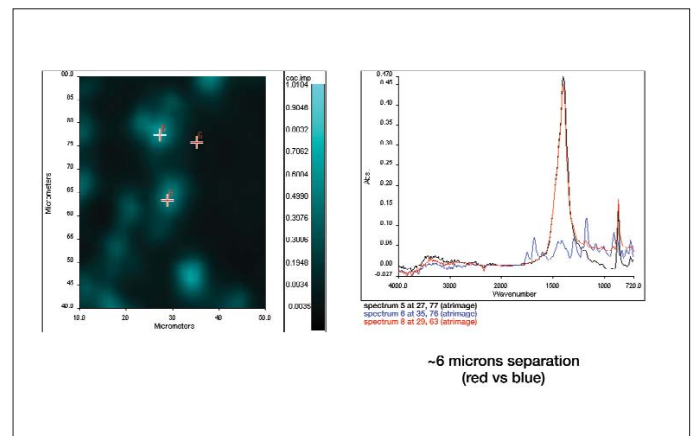


Figure 8e. Exploded view of calcium carbonate image.

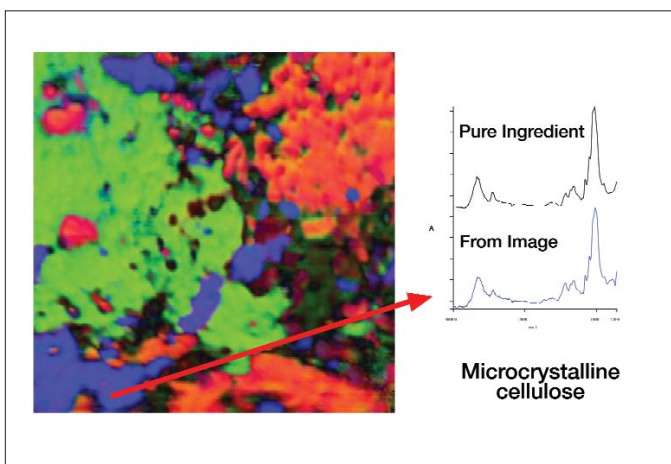


Figure 8c. Overlaying microcrystalline cellulose.

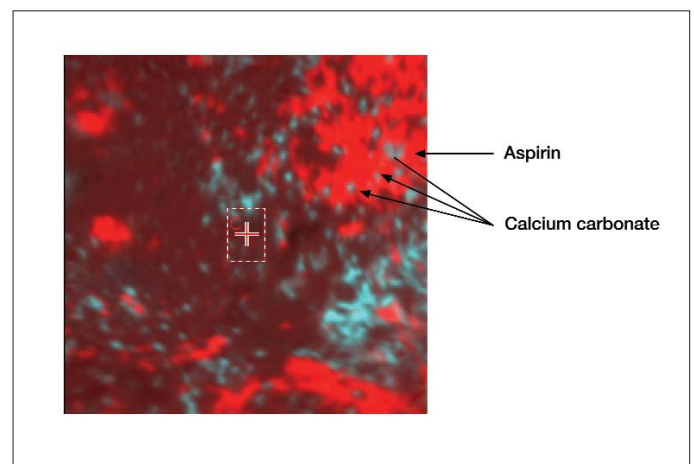


Figure 8f. Calcium carbonate within the aspirin domains.

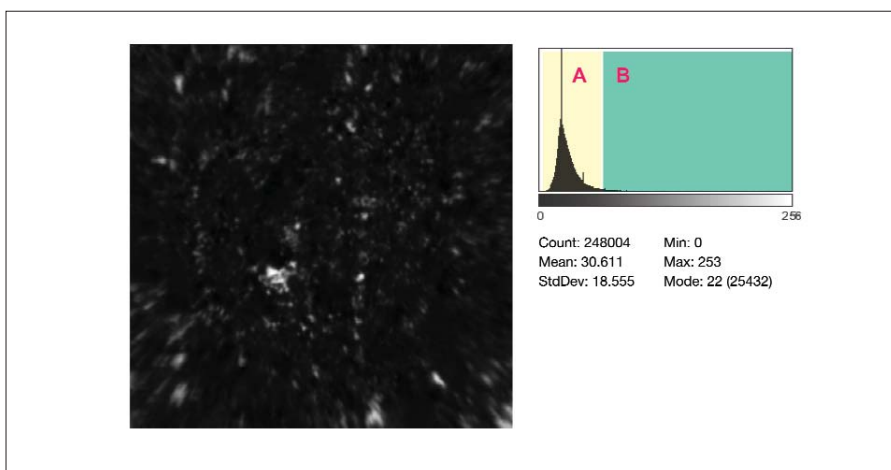


Figure 9a. Individual ingredient distributions as histograms.

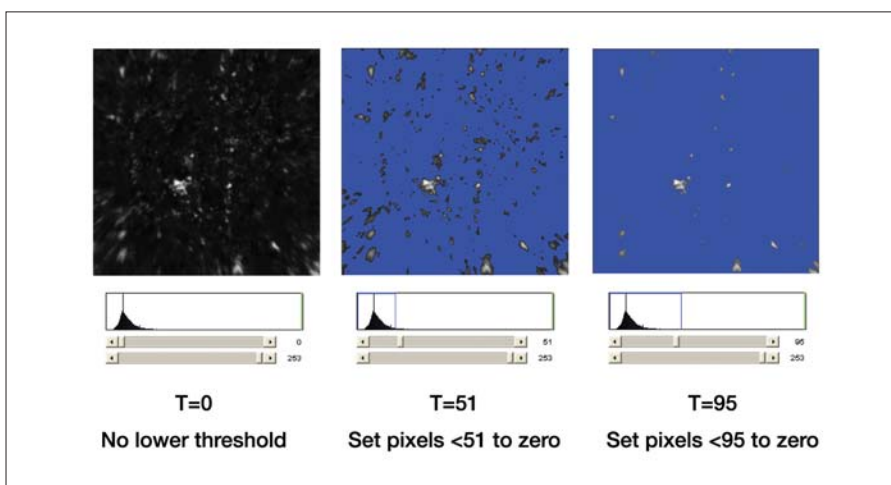


Figure 9b. Setting A-B threshold to produce a binary image.

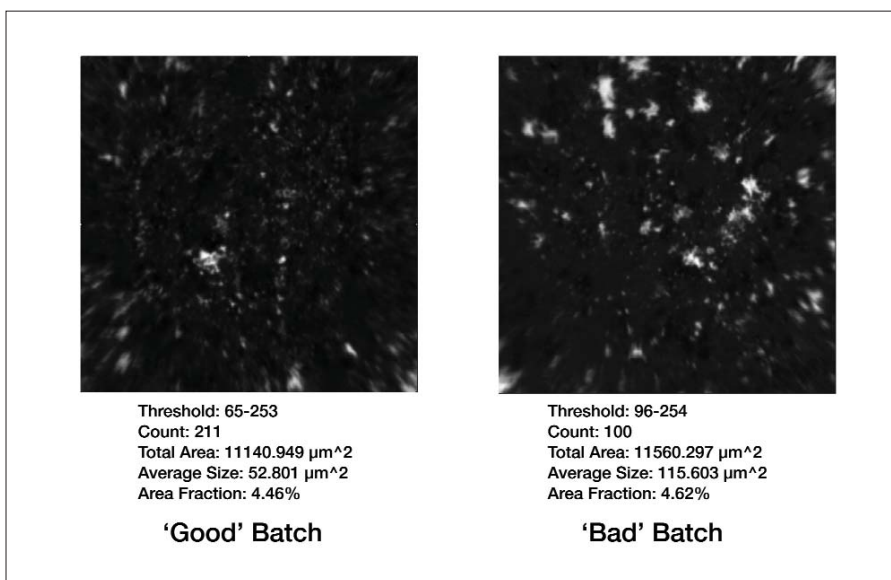


Figure 9c. Some metrics can be related to quality parameters.

been found useful to use a combination of information about the particle size of raw ingredients plus iterative threshold adjustment in conjunction with examination of underlying pixel spectra in order to help establish intensity thresholds.

Figure 9b illustrates thresholding. A component distribution is shown as a calculated grayscale image with intensity thresholds set at two levels to leave the most intense image pixels. Which image is correct? A detailed discussion of this problem is beyond the scope of this note, but the setting of this threshold value is key to deriving accurate quantitative information from these images, and must be used with extreme care. However, when clear distinct particle distributions are calculated, some of the resulting statistics, (e.g. mean particle size, distribution shape, nearest neighbor information, etc.) have been related to product quality attributes. Figure 9c shows calculated ingredient distributions for a given ingredient from two batches of a product labeled 'good' and 'bad'. Five images were recorded from different samples of good and bad batches. For all the ingredients except one the calculated average particle sizes agreed for the good and bad batches. For the remaining ingredient, there was an approximate factor of two difference in average particle size between good and bad batches with all images. Information of this nature can be extremely valuable in helping to establish processing problems.

Conclusion

ATR chemical imaging has advanced the state of the art in chemical imaging of certain types of pharmaceutical tablets. It provides a very

large improvement in achievable spatial resolution compared with NIR chemical imaging, and sharper, generally easier to interpret images. The technique overcomes the major limitation of direct diffuse reflectance imaging in the mid-IR, namely problems with high signal attenuation and uncontrolled specular reflectance contributions in the image. The technique overcomes a number of limitations of Raman imaging such as sample overheating, potential fluorescence, limited spatial resolution (depending on Raman hardware configuration) and relatively long image collection times.

Considering the limitations of the ATR imaging technique, these fall broadly into three areas:

- As a contact technique, once a sample is pressed onto a surface it is effectively contaminated, so crystal cleaning is required before each image is generated. This is, however, relatively fast unless some of the particles of the tablet have strong adhesive properties.

- Small sample penetration depth, so careful experimental design is required to ensure the image at the surface is representative of the sample.
- Given mechanical and optical constraints of the system, the maximum sample area is relatively small (ca 0.5 mm diameter circle with current design) compared with other imaging techniques. Again, design of experiment should take this into consideration.

Despite these limitations, the technique is poised to become a very significant tool in the better understanding of ingredients distributions in pharmaceutical tablets.

REFERENCES

1. Lyon, R.; Lester, D.; Lewis, E. N.; Lee, E.; Yu, L. X.; Jefferson, E. H.; Hussain, A. S.: AAPS PharmSciTech 2002; 3 (3) article 17 (<http://www.aap-spharmscitech.org>).
2. Clarke, F.; Vib Spec., 34 (2004) 25-35. Available online at www.sciencedirect.com.

3. Lewis, E. N.; Schoppelrei, W.; Lee, E.; Kidder, L.; in 'Process Analytical Technology' Blackwell, 2005. ISBN-10 1-4051-2103-3.
4. Canas, A.; Carter, R.; Hoult, R.; Sellors, J.; Williams, S.; 'Spatial resolution in mid-IR ATR Imaging: Measurement and Meaning' FACCS conference, 2006.
5. Rasband, W.S., ImageJ, U. S. National Institutes of Health, Bethesda, Maryland, USA, <http://rsb.info.nih.gov/ij/>, 1997-2006.
6. 'Spatial Resolution in FT-IR ATR Imaging' PerkinElmer Technical Note # 007641_03 (2006).